UDK/*UDC*: 004.942:627.132(047.31)
Izvirni znanstveni članek – *Original scientific paper*
DOI: 10.15292/acta.hydro.2022.08

Prejeto/*Received:* 03.03.2023
Sprejeto/*Accepted:* 09.05.2023
Objavljeno na spletu/*Published online:* 14.06.2023

# FREE-FLOW DISCHARGE CHARACTERISTICS OF AN OVERSHOT GATE: A NON-HYDROSTATIC NUMERICAL MODELING APPROACH

# PRETOČNOST PROSTEGA PRELIVA ČEZ ZAKLOPKO: PRISTOP NEHIDROSTATIČNEGA NUMERIČNEGA MODELIRANJA

**Yebegaeshet T. Zerihun**[1]

[1]David & James – Engineering and Environmental Consultancy, 204 Albion Road, Victoria 3350, Australia

## Abstract

Overshot gates, such as the Lay-flat gate, have been used extensively as a flow-measuring structure in open-channel irrigation conveyance systems. Despite their simple geometric shape, the free flow over such structures possesses a substantial curvature of streamline and a steep free-surface slope, thereby making the assumption of a hydrostatic pressure distribution invalid. Accordingly, the shallow-water approach becomes inapplicable for analyzing their discharge characteristics. Using the depth-averaged Boussinesq-type model, the critical flow conditions based on this lower-order approach were extended, leading to an equation for the free-flow coefficient of discharge that implicitly incorporates the flow's dynamic effects. The developed model was tested for free-flow cases, with a satisfactory agreement between computational results and experimental data. Overall, it was shown that the proposed model is capable of accurately simulating a sharply-curved flow over an overshot gate. The study found that the relative overflow depth prominently affects the characteristics of the curvilinear transcritical flow and hence the free-flow coefficient of discharge. Furthermore, the angle of inclination has a moderate influence on the discharge characteristics of a full-width overshot gate with a face slope flatter than 56°.

**Keywords:** overshot gate, discharge rating curve, pivot weir, non-hydrostatic flow, discharge coefficient, flow measurement.

## Izvleček

Ravne zaklopne zapornice z vrtiščem na spodnjem robu se v veliki meri uporabljajo za merjenje pretoka v namakalnih sistemih z odprtimi kanali. Kljub svoji preprosti obliki ima prosti preliv čez tak objekt precejšnjo ukrivljenost tokovnic in strm naklon gladine, zaradi česar je predpostavka o porazdelitvi hidrostatičnega tlaka neveljavna. Zato je pristop plitvega toka (kot je npr. uporaba po globini povprečenih Navier-Stokesovih enačb) neustrezen za analizo pretočnih karakteristik zaklopke. Z uporabo Boussinesqovega modela povprečne globine so bili pogoji kritičnega toka, ki temeljijo na tem pristopu nižjega reda, razširjeni, kar je privedlo do enačbe za pretočni koeficient prostega preliva, ki implicitno vključuje dinamične učinke pretoka. Razviti model je bil testiran za primere prostega preliva, z zadovoljivim ujemanjem med računskimi rezultati in eksperimentalnimi

[1] Stik / *Correspondence*: zyebegaeshet@gmail.com

podatki. Na splošno se je izkazalo, da je predlagani model sposoben natančno simulirati ostro ukrivljeni tok čez zaklopko. Študija je pokazala, da relativna globina preliva izrazito vpliva na značilnosti ukrivljenega transkritičnega toka in s tem na pretočni koeficient prostega preliva. Poleg tega ima kot naklona zmeren vpliv na pretočne karakteristike zaklopke polne širine pri naklonih manjših od 56°.

**Ključne besede:** zaklopka, pretočna krivulja, vrtilni jez, nehidrostatični tok, pretočni koeficient, merjenje pretoka.

## 1. Introduction

Open channels are commonly used to convey water in the surface irrigation methods. For efficient water management, an adjustable overshot gate such as a pivot weir or a Lay-flat gate is often used to control flow and water levels in these channels. Despite its simple geometric shape, free flow over an overshot gate possesses sharply-curved streamlines with steep slopes. Consequently, the flow field is characterized by the prevalence of non-uniform velocity and non-hydrostatic pressure distributions. As noted by Zerihun and Fenton (2007) and Zerihun (2020), the dynamic effect of a curved-streamline overflow significantly affects the performance of a short-crested type of flow control structure. Apparently, a critical flow theory based on a hydrostatic pressure approach is unsuitable for analyzing such structure's discharge characteristics. The vertical motion of the curvilinear flow must be accounted for by a higher-order numerical model so as to overcome the inherent drawbacks of this conventional approach. Such a non-hydrostatic model allows us to obtain detailed information regarding the complex flow field for a wide range of parameters without resorting to expensive and time consuming experiments. It can also offer insights into the physical processes governing the flow-structure interactions.

The flow characteristics of an overshot gate or a pivot weir with a rectangular control section have been of primary interest to researchers. Bazin (1898) was probably the earliest researcher to investigate the free-flow discharge characteristics of this structure. He performed experiments on overflow structures with angles of inclination varying from 14 to 90°. Since then, extensive experimental studies were carried out to better understand the key characteristics of overflow. Wahlin and Replogle (1994) experimentally studied the hydraulic characteristics of an overshot gate under free- and submerged-flow conditions. For angles of gate inclination between 16 and 55°, they conducted experiments on flows over contracted and full-width overshot gates. They also considered the effect of angle of inclination to extend the equation for the free-flow discharge coefficient of a vertical sharp-crested weir (Kindsvater and Carter, 1957). Likewise, Manz (1985) and Hager (1994) also extended this equation for a similar flow situation. Using dimensional analysis and incomplete self-similarity theory, Di Stefano et al. (2016) developed a stage-discharge relationship for a triangular-shaped weir with a vertical downstream face, which is, obviously, applicable for analyzing the overshot gate flow. By introducing additional correction factors that account for the inadequacies of the lowest-order energy and momentum approaches, Azimfar et al. (2018) developed semi-theoretical equations for free- and submerged-flow discharge coefficients. The submerged-flow characteristics of a similar overflow structure were also experimentally investigated by Bijankhan and Ferro (2020). However, the overall accuracy and application range of the discharge coefficient equations stemming from these studies depend on the scope of the experimental tests. By applying numerical models, the various aspects of free flow over an overshot gate were also investigated. Bijankhan and Ferro (2018) employed the OpenFOAM software, which is based on the Reynolds-averaged Navier-Stokes equations, to examine the influence of the angle of inclination on the discharge characteristics. More recently, the method of smoothed particle hydrodynamics was utilized to analyze the two-dimensional (2D) structure of the gate overflow (Mahdavi and Shahkarami, 2020). In comparison with previous investigation results (e.g. Bazin, 1898; Wahlin and Replogle, 1994); however, this method did not

accurately simulate the trend of the discharge coefficient as a function of the gate slope. Both studies accounted for the effects of a non-hydrostatic pressure distribution.

The literature review demonstrates that most of the above studies devoted empirical methods to develop the discharge coefficient equations rather than applying a critical flow theory based on a non-hydrostatic pressure approach. Furthermore, little effort has been made so far to numerically study the salient features of the curvilinear transcritical flow over an overshot gate. All these deficiencies highlight the need for a comprehensive numerical investigation of the problem of the gate flow. Recently, Zerihun (2017b) developed a depth-averaged Boussinesq-type energy model based on the assumption of a linear variation of streamline geometry parameter across the flow depth. Unlike the governing equations derived from a potential-flow theory (e.g. Fawer, 1937; Matthew, 1991; Homayoon and Jamali, 2021), the model incorporates a higher-order dynamic correction for the effects of the vertical curvatures of the streamline and the steep free-surface slope. Hence, it is eminently suitable for analyzing curvilinear flow problems with continuous free-surface profiles. Similar to the free-overfall problem, the numerical treatment of the free jet part of the overshot gate flow is challenging due to the presence of dual free surfaces. As demonstrated by Zerihun (2004, 2021b), such a problem can be solved by applying both the flow profile and pressure equations with the aid of auxiliary boundary conditions. Therefore, the first aim of the study is to explore the discharge characteristics of a full-width overshot gate under free-flow conditions using a depth-averaged Boussinesq-type model. This also comprises assessing the impacts of the relative overflow depth $h/w$ ($h$ is the overflow depth, and $w$ is the gate height) and angle of inclination on the gate discharge. With the non-hydrostatic model, the lower-order critical flow conditions (Bakhmeteff, 1932, pp. 33-35) are extended to develop an equation for the free-flow coefficient of discharge as in the case of curvilinear flow over a round-crested weir (Fawer, 1937; Hager, 1985; Zerihun, 2017b). Such a physically-based equation can offer a realistic solution to real-life problems related to the accurate prediction of the discharge of a properly ventilated overshot gate from field data. The second aim is to evaluate the performance and applicability of the model in predicting the mean flow characteristics of the curvilinear transcritical flows, including the prominent features of the free jet at the vena contracta. The qualities of the simulation results are thoroughly examined by using a set of experimental data from the literature. It is worth noting that the method presented herein is limited to the analysis of flow over a full-width overshot gate under free-flow conditions. In the following sections, a short summary of the derivation of the governing equations and their numerical solution procedures will be presented first, followed by a discussion of the validation results.

## 2. Numerical modeling methodology

### 2.1 Governing equations

A schematic diagram of free-surface flow over an overshot gate is shown in Figure 1a, in which a subcritical incoming flow becomes a supercritical flow over a short length of the channel. Cartesian coordinates, where $x$ is in the streamwise horizontal direction; $y$ is in the lateral direction; and $z$ is vertically upward, are also shown. It is known that a rapidly-varied transition typically involves a curvilinear flow with substantial vertical curvatures of the streamline that lead to a non-hydrostatic pressure and non-uniform velocity distributions. As noted by Fawer (1937), Montes and Chanson (1998), and Zerihun (2004, 2021a), a higher-order approximation for the vertical distribution of the streamline curvature parameters is necessary in order to accurately treat the complex transition from a hydrostatic to a non-hydrostatic flow regime. By relaxing the weakly-curved flow approximation, Zerihun (2017b) deduced a Boussinesq-type model from the depth-averaged energy equation. For steady flow in a rectangular channel, the equation reads as

$$H_e = \frac{q^2}{2gH^2}\left(\alpha + Z_x^2 + H_x Z_x + \frac{(H_x)^2}{3}\right) + \frac{q^2}{3gH\omega_1} H_{xx} + \frac{q^2 Z_{xx}}{6gH\omega_1}\left(\frac{2\omega_2 + 1}{\omega_2}\right) + \frac{H}{\omega_1} + Z, \tag{1a}$$

$$\frac{dH_e}{dx} = -S_f, \tag{1b}$$

where $H_e$ denotes the total energy head; $H$ is the local flow depth measured vertically; $q$ is the discharge per unit width; $g$ is acceleration due to gravity; $Z_x$ is the local bed gradient of the channel; $S_f$ is the friction slope; $Z_{xx}$ and $H_{xx}$ are the second derivatives of the bed profile and flow depth, respectively; $\omega_1 = 1 + (\eta_x)^2$; $\omega_2 = 1 + (Z_x)^2$; $\eta_x$ is the free-surface slope; $\alpha$ is the Coriolis velocity correction coefficient; and $Z$ is the elevation of the channel bed or the lower nappe of the jet. Equation (1a) is a higher-order depth-averaged equation for 2D hydraulically steep flow problems, where the pressure distribution appreciably deviates from hydrostatic. For quasi-uniform free-surface flows in a constant slope channel ($H_x = H_{xx} = Z_{xx} = 0$ and $\alpha \cong 1.0$), Equation (1a) simplifies to the steep-slope form of the energy equation (Chaudhry, 2022, p. 42), i.e.,

$$H_e = \frac{q^2 \omega_2}{2gH^2} + \frac{H}{\omega_1} + Z. \tag{2}$$

The pressure equation of Zerihun (2017b) for flow in a rectangular channel can be written as follows:

$$\frac{p}{\gamma} = \frac{(1-\zeta)H}{\omega_1} + \frac{q^2 Z_{xx}(1-\zeta)}{gH\omega_1\omega_2} + \frac{q^2}{2gH\omega_1}\left(\eta_{xx} - \frac{Z_{xx}}{\omega_2}\right)(1-\zeta^2), \tag{3a}$$

$$\zeta = \frac{z - Z}{\eta - Z}, \tag{3b}$$

where $\gamma (= \rho g)$ is the unit weight of the fluid; $\rho$ is the density of the fluid; $p$ is the pressure; $\eta$ refers to the free-surface elevation; $z$ is the elevation of a point in the flow field; $\eta_{xx}$ is the second derivative of the free-surface profile; and $\zeta$ is a non-dimensional vertical coordinate. The first term on the right-hand side of Equation (3a) represents the non-hydrostatic pressure due to the effect of the steep free-surface gradient, as noted by Lauffer (1935), while the second and third terms stand for the dynamic component of the pressure due to the effects of the vertical acceleration. In the case of a gradually-varied flow with streamlines nearly parallel to the mild-slope channel, the free-surface and bed curvatures terms vanish ($\eta_{xx} = Z_{xx} \cong 0$ and

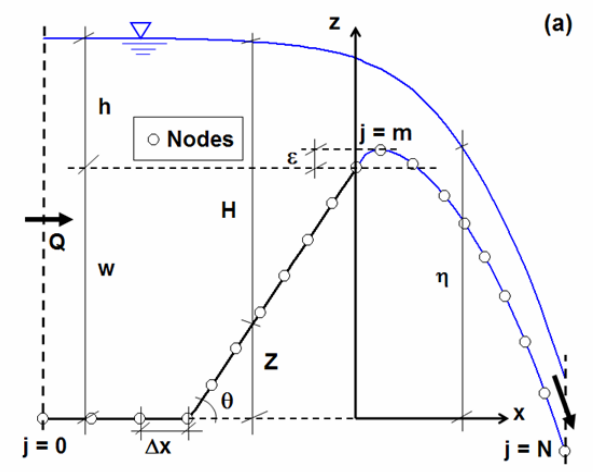



***Figure 1**: (a) Definition sketch and computational domain for the problem of a non-hydrostatic overshot gate flow; and (b) an Obermeyer-type overshot gate system operating under free-flow conditions (Photograph courtesy of Knight Architects, UK). The angle of gate inclination with the horizontal axis is denoted by $\theta$.*

***Slika 1**: (a) Definicijska skica in računska domena za problem nehidrostatičnega toka vode čez zaklopko; in (b) sistem zaklopnih zapornic tipa Obermeyer, brez vpliva spodnje vode (fotografija z dovoljenjem Knight Architects, ZK). Kot naklona zaklopke je označen z $\theta$.*

$\omega_1 = \omega_2 \cong 1.0$), and hence, this equation reduces to a hydrostatic pressure equation. The pressure at the bottom of the channel, $p_b$, can be determined from Equation (3a) by setting $\zeta = 0$ as follows:

$$\frac{p_b}{\gamma} = \frac{H}{\omega_1} + \frac{q^2}{2gH\omega_1}\left(\eta_{xx} + \frac{Z_{xx}}{\omega_2}\right). \tag{4}$$

As a Boussinesq-type energy model, its application is limited to the analysis of rapidly-varied flows with continuous free-surface profiles (see Figure 1b). For the case of flow with a discontinuous free-surface profile such as a hydraulic jump, a higher-order model based on the momentum principle (e.g. Steffler and Jin, 1993; Zerihun, 2017a, 2021a) can be employed to analyze the flow problem without a prior knowledge of the energy dissipation rate. Equations (1a) and (4) will be employed here to analyze the free-flow discharge characteristics of a full-width overshot gate. In these equations, the unknowns are the flow depth, elevation of the lower nappe, and the pressure on the face of the gate. They are numerically determined using an implicit finite-difference scheme. The computed results will be compared with the experimental data in order to examine the validity of the equations for the problem of curvilinear transcritical flow.

### 2.2 Discretized equations and solution method

Equation (1a) is a non-linear ordinary differential equation, and a closed-form solution is available only for idealized cases. Therefore, it is numerically solved by specifying two boundary conditions at the inflow section and at the crest of the gate. The inflow section is located in a hydrostatic flow region, so that a lower-order equation can be applied to compute the total energy head. For the purpose of developing a generalized numerical scheme, Equation (1a) can be rewritten in a form as follows:

$$\lambda_{0,j} H_{xx,j} + \lambda_{1,j}\left(H_{x,j}\right)^2 + \lambda_{2,j} H_{x,j} + \lambda_{3,j} = 0, \tag{5}$$

where the non-linear coefficients $\lambda_{0,j}$, $\lambda_{1,j}$, $\lambda_{2,j}$, and $\lambda_{3,j}$ at node $j$ are defined as

$$\lambda_{0,j} = \frac{q^2}{3gH_j\omega_{1,j}}, \tag{6a}$$

$$\lambda_{1,j} = \frac{q^2}{6gH_j^2}, \tag{6b}$$

$$\lambda_{2,j} = \frac{q^2}{2gH_j^2} Z_{x,j}, \tag{6c}$$

$$\lambda_{3,j} = \frac{q^2\left(\alpha + Z_{x,j}^2\right)}{2gH_j^2} + \frac{q^2 Z_{xx,j}}{6gH_j\omega_{1,j}}\left(\frac{2\omega_{2,j}+1}{\omega_{2,j}}\right) + \frac{H_j}{\omega_{1,j}} + Z_j - \left(H_{e,0} - H_{l,j}\right), \tag{6d}$$

where $H_{e,0}$ is the total energy head at the inflow section, and $H_{l,j}$ is the head loss between the inflow section and a downstream section at node $j$. The first and second spatial derivative terms in Equation (5) were discretized using the four-point finite-difference approximations (Bickley, 1941), which results in the following expression after simplification:

$$\begin{aligned} &36\lambda_{0,j}\left(H_{j-1} - 2H_j + H_{j+1}\right) \\ &+ \lambda_{1,j}\left(H_{j-2} - 6H_{j-1} + 3H_j + 2H_{j+1}\right)^2 \\ &+ 6\Delta x\lambda_{2,j}\left(H_{j-2} - 6H_{j-1} + 3H_j + 2H_{j+1}\right) \\ &+ 36(\Delta x)^2\lambda_{3,j} = 0, \end{aligned} \tag{7}$$

where $\Delta x$ is the size of the step. For the free jet portion, the atmospheric pressure existing on the lower side of the nappe provides an auxiliary boundary condition. Using this fact in Equation (4), the following discretized equation for the lower nappe's elevation was obtained:

$$\begin{aligned} &\left(Z_{j-1} - 2Z_j + Z_{j+1}\right)\left(\frac{\omega_{2,j}+1}{\omega_{2,j}}\right) + \frac{2gH_j^2}{q^2}(\Delta x)^2 \\ &+ \left(H_{j-1} - 2H_j + H_{j+1}\right) = 0. \end{aligned} \tag{8}$$

The above equation was also employed to compute the curvature of the upper nappe profile at the crest of the gate. For simulating the lower nappe profile, the upstream elevation was deduced from the gate height, but its elevation at the downstream end ($j = N$) was specified as an outflow boundary condition. Given that the channel bed did not have curvatures, the discretized form of Equation (5), together with the specified flow depth and atmospheric bed pressure at the inflow section and

at the crest of the gate, respectively, was solved for the upper nappe profile by the Newton–Raphson iterative method with a numerical Jacobian matrix, which proceeded from the assumed initial free-surface position. Based on the relative change in solution criterion with a specified tolerance of $10^{-6}$, the solution error of the numerical scheme was minimized. A similar technique was also applied to predict the lower nappe profile. Further details of the numerical procedures for the problem of dual free-surfaces flow can be found in Zerihun (2004, 2021b).

### 2.3 General remarks on model application

In the next section, the accuracy of the proposed model will be systematically examined by comparing its solutions for the problems of an overshot gate flow with the experimental data. Using the criteria proposed by Hager (2010, p. 291) and Curtis (2016), the effects of surface tension and viscosity on the experimental data were examined. Accordingly, experimental data with $h/w \geq 0.1$ and $h \geq 50$ mm were considered for calibration and validation purposes. In the numerical model, the energy loss due to friction was estimated using the Darcy–Weisbach equation with an explicit form of the Colebrook–White formula (Zigrang and Sylvester, 1982) for the friction factor. In this method, the effect of the steep gradient of the bed on flow resistance was taken into account by considering a drag force tangent to the bed (Berger, 1994), which led to a resistance equation with a parameter for the wetted perimeter in a plane normal to the bed. Additionally, the Coriolis coefficient, $\alpha$, was computed using Zerihun's (2004) numerical procedure from the experimental data of Rajaratnam and Muralidhar (1971) and Tim (1986) for free flow over a vertical sharp-crested weir. The result indicated a minimum value of 1.01 near the inflow section and a maximum value of 1.2 in the curvilinear flow region. During the simulations, its value was varied between these extremes along the computational nodes.

### 2.4 Results of the model validations

The results of the numerical model for free-surface and bottom-pressure profiles were validated using the test data presented by U.S. Bureau of Reclamation [USBR] (1948). Some of the USBR's experimental work was done on flows over inclined sharp-crested weirs, which are similar to flows over overshot gates. Under free-flow conditions, weirs with angles of inclination varying from 45 to 90º and spanning the full width of the flume were tested. The pressure on the face of the weir and the profiles of the nappe shapes were measured by piezometers and coordinometers, respectively. The measurements were accurate to 0.3 mm. Figure 2 shows the free-surface profiles and the pressure on the upstream face of the gate. In this figure, the normalized free-surface elevation $\Omega\,(=\eta/\eta_0)$ and the normalized pressure on the gate face $\xi = p_b/\gamma h$ are plotted against the normalized horizontal distances $X\,(=x/\eta_0)$ and $X_w\,(=x/h)$, respectively, where $\eta_0$ is the elevation of the free surface at the inflow section. In the supercritical flow region where the streamlines have steep slope and substantial vertical curvatures, the model satisfactorily predicted the free-surface elevations of the upper and lower nappes. Upstream of the crest of the gate, the model correctly reproduced the free-surface profiles, and its results matched reasonably well with the experimental data (see Figure 2a-c). As can be seen from Figure 2d, the trend of the profile of the pressure on the face of the overshot gate was correctly simulated, but the predicted values were slightly lower than the measured ones. The good correlation between the numerical results and experimental data demonstrates the suitability of the proposed model for simulating non-hydrostatic transcritical flows over overshot gates.

### 2.5 Crest of the lower nappe profile

Information on the location of the crest of the lower nappe is vital for the application of a critical flow theory. As described by Jaeger (1956, p. 134), critical flow conditions can occur only at this local maximum of the bottom profile. Because of this fact, the effects of the angle of inclination and relative overflow depth on the maximum height of

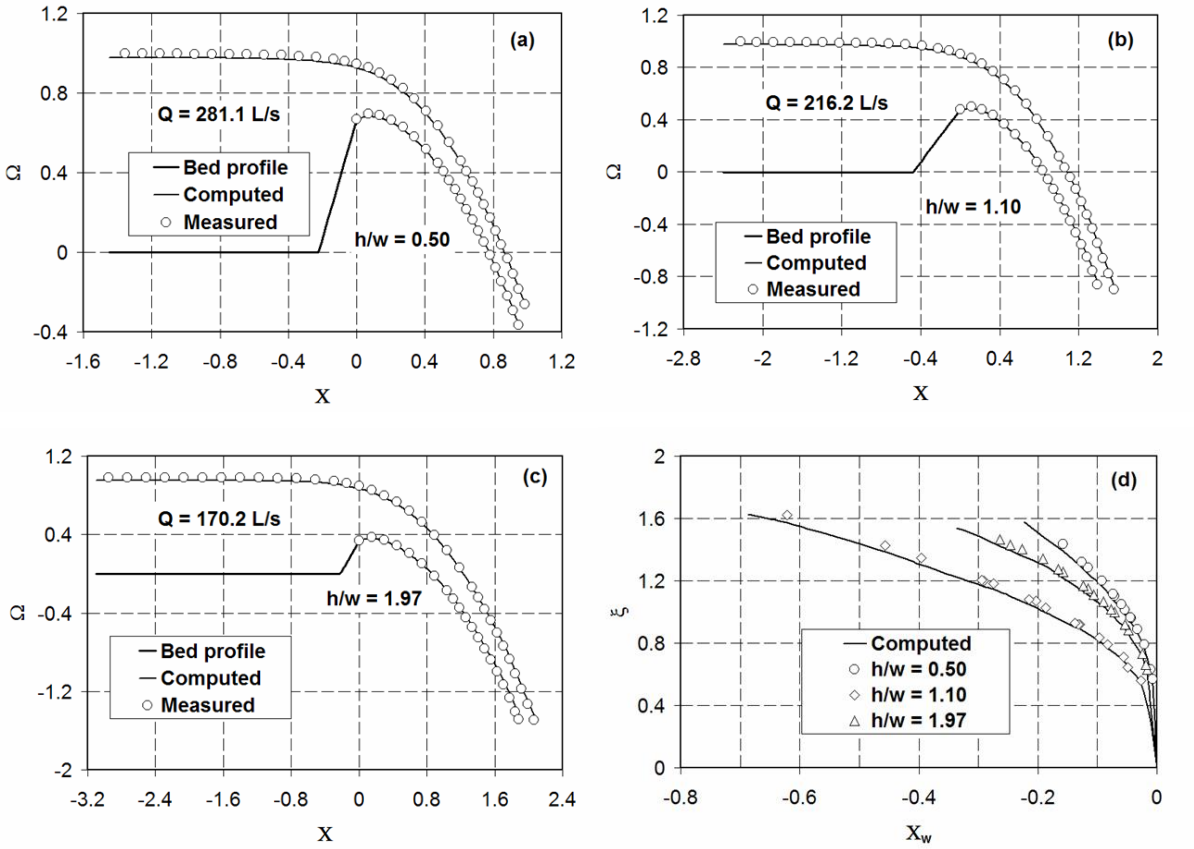


***Figure 2:*** *Normalized free-surface profiles for curvilinear transcritical flows over overshot gates: (a)* $\theta = 71.57^\circ$ *; (b)* $\theta = 45.0^\circ$ *; and (c)* $\theta = 56.31^\circ$ *. The corresponding pressure profiles in (d) are along the centerline of the face of the gate. The numerical results are compared with the experimental data of USBR (1948).*

***Slika 2:*** *Normalizirani profili proste gladine za ukrivljene transkritične tokove čez zaklopko: (a)* $\theta = 71.57^\circ$ *; (b)* $\theta = 45.0^\circ$ *; in (c)* $\theta = 56.31^\circ$ *. Ustrezni profili tlaka v (d) so vzdolž središčne črte sprednje strani zaklopne zapornice. Prikazana je primerjava rezultatov numeričnega modela z eksperimentalnimi podatki USBR (1948).*

this nappe above the gate crest were examined by analyzing the numerical results and the test data of Bazin (1898) and USBR (1948). Figure 3a shows the variation of the relative maximum height of the lower nappe $\varepsilon / w$ with the relative overflow depth $h / w$. Since the magnitude of the discharge influences the slope of the lower nappe at the gate crest, its relative maximum height decreases as the relative overflow depth increases. For a constant $h / w$, the relative maximum height increases with increasing angle of inclination, as depicted in Figure 3b. The trend of the analyzed data can be expressed as follows:

$$\frac{\varepsilon}{h} = -0.005\frac{h}{w} + 0.112\theta^{0.671} - 0.046. \qquad (9a)$$

The coefficient of determination ( $r^2$ ) leading to the above equation is 0.94. Likewise, the variation of the location of the vena contracta (flow section at the crest of the lower nappe) was examined, and the following regression equation ( $r^2 = 0.98$ ) is obtained:

$$X_m = 0.199\frac{h}{w} + 22.936\,\theta^{0.003} - 22.912, \qquad (9b)$$

where $X_m (= x_m / h)$ is the normalized horizontal distance of the vena contracta from the gate crest. Equations (9a) and (9b) are the results of a regression analysis based on a non-linear optimization approach (Lasdon et al., 1974). In both equations, the angle of inclination $\theta$ is in radian. As shown in Figure 4, the relative overflow depth and angle of inclination influence the relative position of the vena contracta. Its position shifts further downstream as the relative overflow depth increases. A similar trend can also be seen as the gate slope becomes steeper. The results of the analysis for the key features of the lower nappe profile are consistent with the results of the Kandaswamy and Rouse (1957) investigation on flow over a vertical sharp-crested weir. In the next section, the capability of the depth-averaged Boussinesq-type model for developing the free-flow discharge rating curve of an overshot gate will be examined.

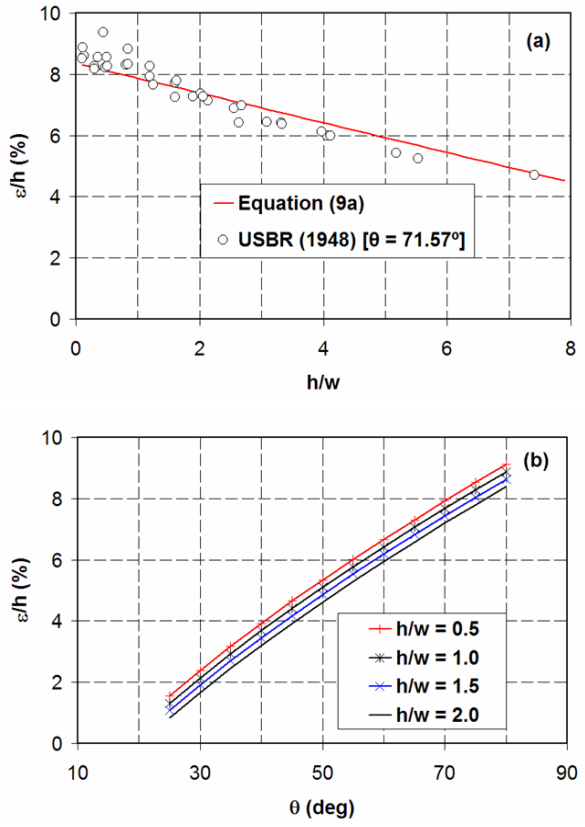


***Figure 3:*** *(a) Correlation between the relative maximum height of the lower nappe and the relative overflow depth; and (b) variation of the relative maximum height of the lower nappe with the angle of inclination for various values of* $h/w$.

***Slika 3:*** *(a) Korelacija med relativno največjo višino spodnjega obrisa curka in relativno prelivno višino; in (b) spreminjanje relativne največje višine spodnjega obrisa curka s kotom naklona za različne vrednosti* $h/w$.

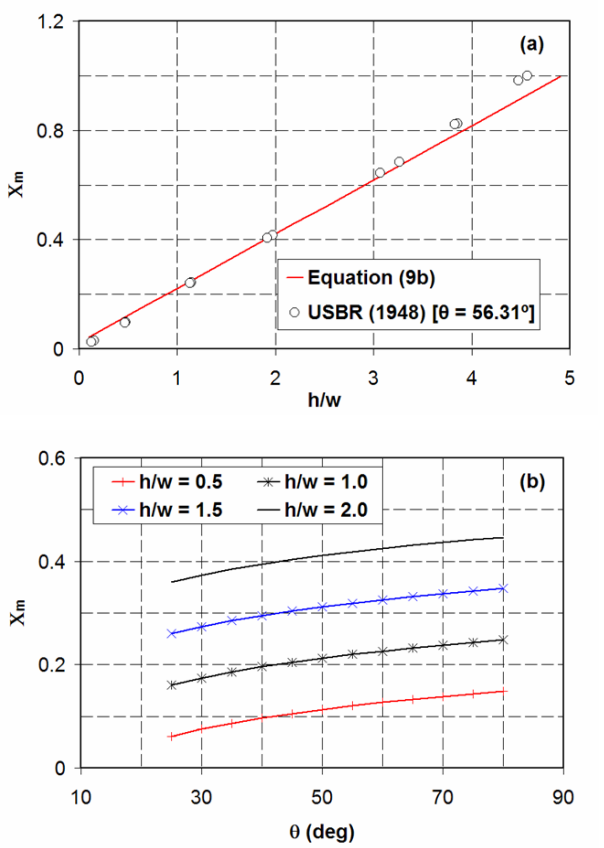


***Figure 4:*** *(a) Correlation between the location of the vena contracta and the relative overflow depth; and (b) variation of the position of the vena contracta with the angle of inclination for various values of* $h/w$.

***Slika 4:*** *(a) Korelacija med lokacijo vene kontrakta in relativno prelivno višino; in (b) sprememba položaja vene kontrakta s kotom nagiba zapornice za različne vrednosti* $h/w$.

## 3. Head-discharge relationship

### 3.1 Free-flow coefficient of discharge

A critical flow theory based on a non-hydrostatic pressure approach is applied here to develop an equation for the discharge coefficient. For this purpose, the lower nappe profile is treated as a bed of a channel in which its elevation varies with the

hydraulic conditions of the flow. Unlike a rigid or a movable bed channel, the atmospheric pressure along its profile provides an auxiliary boundary condition. As noted by Rouse (1936), conditions of critical flow occur at the maximum elevation of the lower nappe profile ($Z_x \cong 0$ and $\omega_2 = 1$), and hence, the flow attains its minimum specific energy (Bakhmeteff, 1932, p. 35). Using such conditions for the critical flow problem of an overshot gate, the relationship between the minimum specific energy $E\left(= H_e - Z\right)$ and the critical depth can be obtained by differentiating Equation (1a) with respect to $H$, while the discharge is kept constant. Mathematically, this can be expressed as

$$\frac{dE}{dH} = 1 - \frac{q^2}{gH_m^2}\Gamma_1 - \frac{q^2}{gH_m^3}\Gamma_3 + \frac{q^2}{gH_m}\frac{d\Gamma_1}{dH} = 0, \quad (10a)$$

$$\Gamma_1 = \frac{H_{xx}}{3} + \frac{Z_{xx}}{2} = -\left(\frac{2R_b\omega_1^{3/2} + R_s}{6R_bR_s}\right), \quad (10b)$$

$$\Gamma_3 = \omega_1\left(\alpha + \frac{\left(H_x\right)^2}{3}\right), \quad (10c)$$

where $R_b$ and $R_s$ are the radii of curvature of the streamline at the lower and upper nappes, respectively, and $H_m$ is the critical flow depth at the crest of the lower nappe profile. A closure relation for the above equation can be obtained by applying the auxiliary boundary condition at $j = m$. Using this condition in Equation (4), the following expression is obtained:

$$R_b = \frac{q^2R_s}{2gH_m^2R_s - \omega_1^{3/2}q^2}. \quad (11)$$

Equation (10a) is a higher-order equation for critical flow depth, which accounts for the effects of a non-hydrostatic pressure distribution. If the geometric characteristics of the streamline at the upper nappe are known in addition to the flow parameters, then this equation gives a useful solution to the problem of the curvilinear critical flow. Substituting Equation (11) into Equation (10b) and simplifying the resulting expression yields an equation independent of $R_b$ as follows:

$$\Gamma_1 = -\left(\frac{\omega_1^{3/2}}{6R_s} + \frac{gH_m^2}{3q^2}\right). \quad (12)$$

As mentioned before, a critical flow approach based on a non-hydrostatic pressure can offer tangible solutions to real-life flow problems, provided that the position of a channel section for critical depth computation is known in advance. For the problem of free-surface flow considered, Equation (10a) can be rewritten as

$$H_m^3 + \frac{3q^2}{2g}\frac{d\Gamma_2}{dH}H_m^2 - \frac{3q^2\Gamma_2}{2g}H_m - \frac{3q^2}{2g}\Gamma_3 = 0, \quad (13a)$$

$$\Gamma_2 = -\frac{\omega_1^{3/2}}{6R_s}, \quad (13b)$$

$$\frac{d\Gamma_2}{dH} \cong \frac{2gR_b\omega_1^{3/2}}{3q^2R_s}\left(H_m + 2R_b\right). \quad (13c)$$

In the above equation, the value of $\Gamma_3$ is always positive. However, the sign of the value of $\Gamma_1$ depends on the shape of the streamline's vertical curvature. For convex free-surface flows such as free flow over an overshot gate, $\Gamma_1$ is always a negative quantity, and $\Gamma_2$ is too. For this type of flow, Equation (13a) has only one real-valued positive root for critical flow depth, and it can be found by applying an iterative numerical procedure based on the bisection method that proceeds from the estimated value of $R_b$. Using this flow depth, the specific energy of the flow at $j = m$ ($E_m$) can be computed from Equation (1a), i.e.,

$$E_m = \frac{q^2}{\omega_1 gH_m}\Gamma_2 + \frac{q^2}{2\omega_1 gH_m^2}\Gamma_3 + \frac{2H_m}{3\omega_1}. \quad (14)$$

From a practical perspective, the discharge equation of an overflow structure can be expressed as a function of the upstream crest-referenced flow depth (see, e.g. Horton, 1907; Bos, 1989, p. 47). Thus,

$$q = \frac{2}{3}C_D\sqrt{2g}h^{3/2}, \quad (15)$$

where $C_D$ is the discharge coefficient. Accurately describing the discharge characteristics of an overshot gate requires the application of an equation

that accounts for the effects of the streamline vertical curvature and steep free-surface slope. Inserting Equation (15) into Equation (14) yields the desired expression for the discharge coefficient as follows:

$$C_D = \frac{3}{2\sqrt{3}}\left(\frac{H_m}{h}\right)^{3/2}\left(\frac{3\omega_1\left(\frac{E_m}{H_m}\right)-2}{2H_m\Gamma_2+\Gamma_3}\right)^{1/2} . \quad (16)$$

As $h/w \to +\infty$, the gate flow exhibits the features of a plane free overfall. For this type of flow, the above equation can be applied to describe the discharge characteristics after some mathematical manipulation following the Rouse (1936) approach. A simplified computational approach based on a sound theoretical basis is applied here to solve the above non-linear algebraic equations. It is apparent that the magnitude of the relative overflow depth influences the degree of the vertical curvature of the streamline. This non-dimensional parameter has a prominent effect on the free-flow discharge characteristics, and hence, it has to be implicitly incorporated in the above equation. By systematically analyzing the experimental data of Bazin (1898) and USBR (1948) using a non-linear optimization technique, the following empirical equations ($0.84 \le r^2 \le 0.99$) were developed for the various parameters appearing in Equation (16):

$$\frac{E_m}{H_m} = 0.001\frac{h}{w} + 0.013\theta^{0.580} + 1.013, \quad (17a)$$

$$\frac{H_m}{h} = 0.092\left(\frac{h}{w}\right)^{0.499} + 0.733\theta^{-0.102}, \quad (17b)$$

$$\Gamma_2 H_m = -0.003\ln\left(\frac{h}{w}\right) + 0.003\theta^{2.150} - 0.074, \quad (17c)$$

where $\theta$ is in radian. All the regression equations developed here are valid for $0.1 \le h/w < 6.5$ and for $26^\circ \le \theta < 90^\circ$. The results of the validation for selected parameters are depicted in Figure 5. As can be seen, the computed results agreed closely with those values determined from the experimental data of Wahlin and Replogle (1994) for a full-width overshot gate. It can be shown from the above equations that for a small angle of inclination ($\theta < 30^\circ$) and $h/w > 5$, the gate flow becomes a sill flow with a critical section in the channel of approach, as previously noted by Böss (1929). For a similar overflow structure with a face slope stepper than 70º, however, the relative overflow depth can reach an upper limit value of 10, which is regarded as the borderline between the two types of flows (Kandaswamy and Rouse, 1957). Compared to the non-hydrostatic method developed here, the earlier empirical approaches (e.g. Hager, 1994; Wahlin and Replogle, 1994; Azimfar et al., 2018; Bijankhan and Ferro, 2018) did not employ higher-order critical flow conditions.

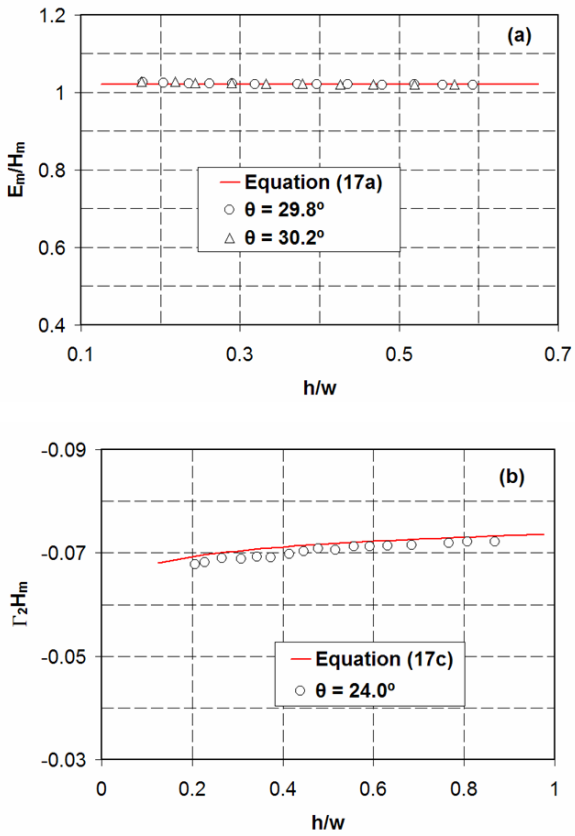


***Figure 5:*** *Variations of the (a) relative specific energy head and (b) curvature of the free surface with the relative overflow depth.*

***Slika 5:*** *Variacije (a) relativne specifične energijske višine in (b) ukrivljenosti proste gladine z relativno prelivno višino.*

### 3.2 Results and discussion

In Figure 6, the discharge coefficients computed from the present method were compared against the

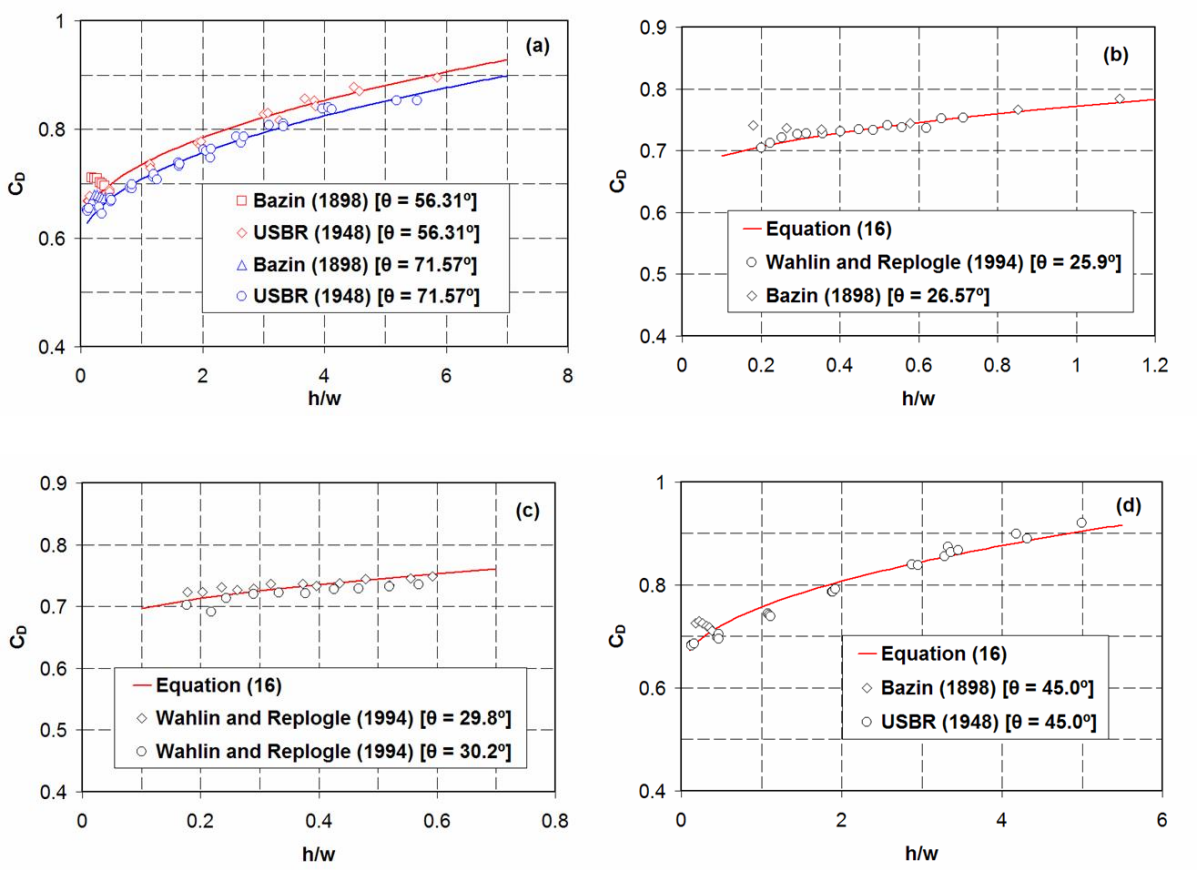


***Figure 6:*** *Comparison of predicted and measured discharge coefficients for overshot gates discharging under free-flow conditions. The results of Equation (16) in (a) are shown in solid lines with the colors of the corresponding experimental data.*

***Slika 6:*** *Primerjava predvidenih in izmerjenih pretočnih koeficientov zaklopke za primer prostega preliva. Rezultati enačbe (16) v (a) so prikazani z neprekinjeno črto z barvami ustreznih eksperimentalnih podatkov.*

experimental data of Bazin (1898), USBR (1948), and Wahlin and Replogle (1994). The results reasonably follow the trend of the experimental data over a large range of $h/w$. The maximum absolute relative errors of the numerical results vary from 2.12 to 5.84%. The influence of the vertical curvature of the streamline on the discharge characteristics is dominant under free-flow conditions. As depicted in Figures 6 and 7, the discharge coefficient increases with increasing the relative overflow depth for the range of gate operation considered. It attains its maximum value at a gate slope of about 34º. Compared to a vertical sharp-crested weir flow, the discharge coefficients of the overshot gates with $\theta = 30.0, 45.0, 56.31$, and $71.57^\circ$ are increased on average by 14.2, 10.9, 7.6, and 3.7%, respectively. Such differences between the capacities of these structures are attributed to the fact that, with a flatter angle of inclination, the energy-dissipating corner eddies on the upstream side of the gate consume less energy. The result indicates that, for $\theta > 56.0^\circ$, the discharge coefficient of the gate deviates from the corresponding value of the vertical sharp-crested weir by less than 6% due to the large size energy-dissipating eddies in the recirculation zone. This implies that, for a steeply sloping gate, the angle of inclination slightly influences the free-flow coefficient of discharge. As a measure of its hydraulic efficiency, the average relative discharge of the overshot gate $\psi (= q/q_v$, where $q_v$ is the unit discharge of a vertical sharp-crested weir) was computed for different gate slopes and is shown in Figure 8. The maximum $\psi$ was found to be 1.14, quite close to the results of previous investigations

(e.g. Manz, 1985; Wahlin and Replogle, 1994). The relative discharge result of Wahlin and Replogle (1994) is based on the data of a contracted gate flow. This might be the cause for their result's deviation from the prediction of the present method, especially for $\theta$ between 60 and 90º.

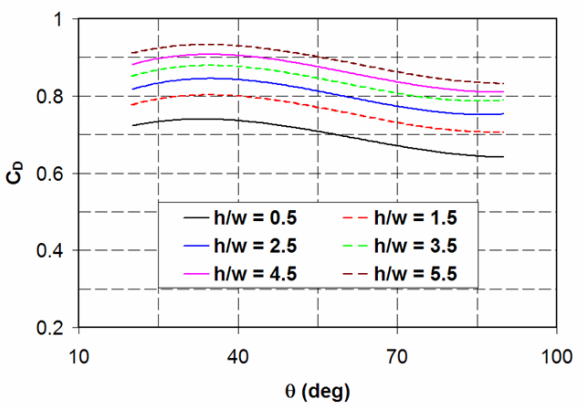


***Figure 7:*** *Discharge coefficient as a function of the angle of inclination for various values of* $h/w$.

***Slika 7:*** *Pretočni koeficient v odvisnosti od kota nagiba za različne vrednosti* $h/w$.

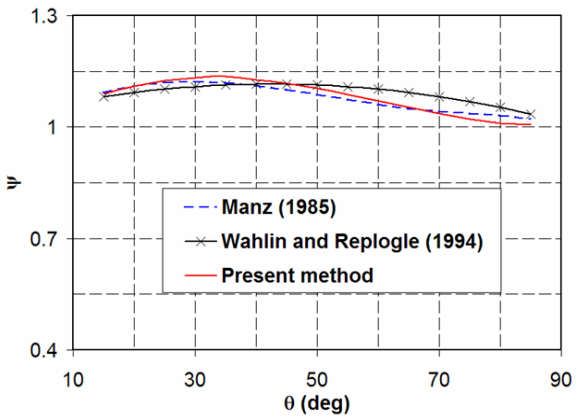


***Figure 8:*** *Variation of the relative discharge* $\psi$ *with the angle of gate inclination* $\theta$.

***Slika 8:*** *Sprememba relativnega pretoka* $\psi$ *s kotom naklona zapornice* $\theta$.

The computed discharge based on Equation (16) was also compared with the results of the empirical equations proposed by Hager (1994) and Wahlin and Replogle (1994). Both studies considered the effect of angle of inclination and extended the discharge coefficient equation of Kindsvater and Carter (1957), which was developed for free flow over a vertical sharp-crested weir. The modified Hager (1994) equation can be written as follows:

$$Q = C_D B\sqrt{2g}H_0^{3/2}, \tag{18a}$$

$$C_D = \frac{2}{3}C_{DV} + 0.05\sin\left(\frac{3}{2}(90-\theta)\right), \tag{18b}$$

where $Q$ is the discharge; $H_0(=E_0-w)$ is the upstream energy head with reference to the gate crest; and $C_{DV}$ is the discharge coefficient of a vertical sharp-crested weir (Kindsvater and Carter, 1957), which is given by

$$C_{DV} = 0.075\frac{h}{w} + 0.602. \tag{18c}$$

Using a correction factor for the angle of inclination ($C_C$), Wahlin and Replogle (1994) proposed the following discharge equation:

$$Q = \frac{2}{3}C_C C_{DV} B\sqrt{2g}\,h^{3/2}, \tag{19a}$$

$$C_C = 1.0333 + 3.848\times10^{-3}\theta - 4.5\times10^{-5}\theta^2. \tag{19b}$$

As described before, the selected experimental data are free of size-scale effects attributed to viscosity and surface tension. Therefore, a correction factor for such effects is not necessary for the above empirical equations. Also, the angle $\theta$ in these equations is in degrees. As shown in Figure 9, the computed discharges $Q_C$ using the three methods compare satisfactorily with the experimentally determined discharges $Q_E$. All computed results fell within the error bandwidth of ±10%. The mean absolute relative errors are 2.3, 3.0, and 2.8% for the present, Hager (1994), and Wahlin and Replogle (1994) methods, respectively. This indicates that the performance of the proposed method is marginally better than the earlier methods. It is also capable of predicting the discharge coefficient of the gate with an accuracy of ±6%. The overall computational results confirmed that the non-hydrostatic method presented here is efficient and accurate in modeling the discharge characteristics of an overshot gate under free-flow conditions.

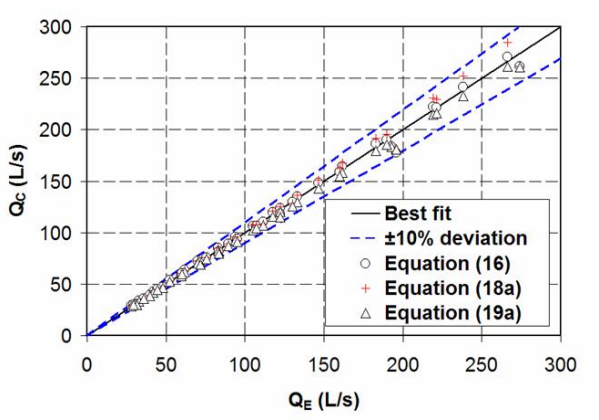


***Figure 9:*** *Comparison of discharges computed by different methods with the experimental data of Bazin (1898) and Wahlin and Replogle (1994) for free flows over full-width overshot gates.*

***Slika 9:*** *Primerjava pretokov, izračunanih z različnimi metodami, z eksperimentalnimi podatki Bazin (1898) ter Wahlin in Replogle (1994) za prosti preliv čez zaklopno zapornico polne širine.*

## 4. Conclusions

The free flow and discharge characteristics of a full-width overshot gate were investigated using a depth-averaged Boussinesq-type energy model. With this model, the critical flow conditions based on the hydrostatic pressure approach were extended and then applied to develop an equation for the free-flow coefficient of discharge. To simplify the numerical computations, empirical equations for relevant flow parameters were developed by applying a non-linear optimization technique. These equations are valid for $0.1 \le h/w < 6.5$ and for $26^\circ \le \theta < 90^\circ$. The results of the computation for local flow characteristics were verified using a set of experimental data from the literature.

For the problems of an overshot gate flow, the model accurately predicted the free-surface profiles, including the transition from a hydrostatic to a non-hydrostatic flow regime. Compared to the measurements, however, it slightly underestimated the pressure on the face of the overshot gate. In general, the proposed model is suitable for simulating curvilinear transcritical flow with dual free surfaces, in which the effects of the dynamic pressure and steep slope are significant.

Using Equation (16), the free-flow discharge coefficient of an overshot gate flow was computed and validated. The results of the validation confirmed that the equation can be used to predict the discharge coefficient with an accuracy of approximately ±6%. Close examination of the simulation results reveals the high dependence of this structure's discharge coefficient on the relative overflow depth, which is a measure of the degree of the overflowing nappe's vertical curvature. In addition, the angle of inclination moderately affects the discharge characteristics of the gate with a face slope flatter than 56°. Its impact on the discharge of a steeply sloping gate is marginal. The proposed numerical method for predicting the coefficient of discharge under free-flow conditions can be extended and implemented for other types of overflow structures, in which the curvilinearity of the streamline strongly influences their discharge characteristics.

## References

Azimfar, S. M., Hosseini, S. A., Khosrojerrdi, A. (2018). Derivation of discharge coefficient of a pivot weir under free- and submerged-flow conditions. *Flow Meas. Instrum*., 59, 45–51.

Bakhmeteff, B. A. (1932). *Hydraulics of Open Channels*. 1st ed.; McGraw-Hill, New York, NY, USA.

Bazin, H. (1898). *Expériences Nouvelles sur L'écoulement en Déversoir (Recent Experiments on the Flow of Water over Weirs)*. Dunod: Paris, France [in French].

Berger, R. C. (1994). Strengths and weaknesses of shallow-water equations in steep open-channel flow. *In: Proceedings of the National Conference on Hydraulic Engineering*, *ASCE*, Buffalo, NY, USA, 1–5 Aug., 2, 1257–1262.

Bickley, W. G. (1941). Formulae for numerical differentiation. *Math. Gaz*., 25(263), 19–27, https://doi.org/10.2307/3606475.

Bijankhan, M., Ferro, V. (2018). Experimental study and numerical simulation of inclined rectangular weirs. *J. Irrig. Drain. Eng*., 144(7), https://doi.org/10.1061/(ASCE)IR.1943-4774.0001325.

Bijankhan, M., Ferro, V. (2020). Experimental modeling of submerged pivot weir. *J. Irrig. Drain. Eng.*, 146(3), https://doi.org/10.1061/(ASCE)IR.1943-4774.0001455.

Böss, P. (1929). Berechnung der abflussmengen und der wasserspiegellage bei abstürzen und schwellen, unter besonderer berücksichtigung der dabei auftretenden zusatzspannungen (Computation of discharges and water level in the event of falls and rises, taking into account the additional pressures that occur). *Wasserkraft und Wasserwirtschaft,* 24(2), 13–14; 24(3), 28–33 [in German].

Bos, M. G. (1989). *Discharge Measurement Structures*. 3rd rev. ed.; International Institute for Land Reclamation and Improvement: Wageningen, The Netherlands.

Chaudhry, M. H. (2022). *Open-Channel Flow*. 3rd ed.; Springer Nature Switzerland AG, Cham, Switzerland.

Curtis, K. W. (2016). *Size-Scale Effect on Linear Weir Hydraulics*. Master's Thesis, Utah State University, Logan, UT, USA.

Di Stefano, C., Ferro, V., Bijankhan, M. (2016). New theoretical solution of the outflow process for a weir with complex shape. *J. Irrig. Drain. Eng.*, 142(10), https://doi.org/10.1061/(ASCE)IR.1943-4774.0001045.

Fawer, C. (1937). *Etude de Quelques Écoulements Permanents à Filets Courbes (Study of Some Permanent Flows with Curved Filaments)*. Docteur ès Sciences Techniques Thèse, Université de Lausanne, Lausanne, Switzerland [in French], https://doi.org/10.5075/epfl-thesis-9.

Hager, W. H. (1985). Critical flow condition in open-channel hydraulics. *Acta Mech.*, 54(3–4), 157–179.

Hager, W. H. (1994). Dammüberfälle (Dam overflows). *Wasser und Boden*, 45(2), 33–36 [in German].

Hager, W. H. (2010). *Wastewater Hydraulics–Theory and Practice*. 2nd ed.; Springer-Verlag: Berlin Heidelberg, Germany.

Homayoon, L., Jamali, M. (2021). Non-hydrostatic formulation of unsteady single and two-layer flow over topography. *J. Hydraul. Eng.*, 147(2), https://doi.org/10.1061/(ASCE)HY.1943-7900.0001826.

Horton, R. E. (1907). *Weir Experiments, Coefficients, and Formulas*. Water-Supply and Irrigation Paper No. 200, U.S. Geological Survey, Government Printing Office, Washington, DC, USA.

Jaeger, C. (1956). *Engineering Fluid Mechanics*. Blackie and Son Limited, London and Glasgow, UK.

Kandaswamy, P. K., Rouse, H. (1957). Characteristics of flow over terminal weirs and sills. *J. Hydraul. Div.*, 83(HY4), 1–13.

Kindsvater, C. E., Carter, R. W. (1957). Discharge characteristics of rectangular thin-plate weirs. *J. Hydraul. Div.*, 83(HY6), 1–36.

Lasdon, L. S., Fox, R. L., Ratner, M. W. (1974). Non-linear optimization using the generalized reduced gradient method. *Revue Fr. d'Automatique Inform. Rech. Opér.*, 3(8), 73–103.

Lauffer, H. (1935). Druck, energie und fliesszustand in gerinnen mit grossen gefälle (Pressure, energy, and flow conditions in channels with high gradients). *Wasserkraft und Wasserwirtschaft*, 30(7), 78–82 [in German].

Mahdavi, A., Shahkarami, N. (2020). SPH analysis of free-surface flow over pivot weirs. *KSCE, J. Civ. Eng.*, 24(4), 1183–1194.

Manz, D. H. (1985). *Systems Analysis of Irrigation Conveyance Systems.* Ph.D. Thesis, University of Alberta, Edmonton, AB, Canada.

Matthew, G. D. (1991). Higher order, one-dimensional equations of potential flow in open channels. *Proc. Instn. Civ. Eng.*, 91(3), 187–201.

Montes, J. S., Chanson, H. (1998). Characteristics of undular hydraulic jumps. Experiments and analysis. *J. Hydraul. Eng.*, 124(2), 192–205.

Rajaratnam, N., Muralidhar, D. (1971). Pressure and velocity distributions for sharp-crested weirs. *J. Hydraul. Res.*, 9(2), 241–248.

Rouse, H. (1936). Discharge characteristic of the free overfall: Use of crest section as a control provides easy means of measuring discharge. *ASCE, Civ. Eng.*, 6(4), 257–260.

Steffler, P. M., Jin, Y. (1993). Depth averaged and moment equations for moderately shallow free-surface flow. *J. Hydraul. Res.*, 31(1), 5–17.

Tim, U. S. (1986). *Characteristics of Some Hydraulic Structures Used for Flow Control and Measurement in Open Channels*. Ph.D. Thesis, Concordia University, Montreal, QC, Canada.

U.S. Bureau of Reclamation. (1948). *Studies of Crests for Overfall Dams*. Hydraulic Investigations, Bulletin 3, Part VI, Boulder Canyon Project Final Reports, Denver, CO, USA.

Wahlin, B. T., Replogle, J. A. (1994). *Flow Measurement Using an Overshot Gate*. Research Report, Cooperative Agreement No. 1425-2-FC-81-19060, U.S. Department of the Interior Bureau of Reclamation, Denver, CO, USA.

Zerihun, Y. T. (2004). *A One-Dimensional Boussinesq-Type Momentum Model for Steady Rapidly-Varied Open-*

*Channel Flows*. Ph.D. Thesis, The University of Melbourne, Melbourne, Vic, Australia.

Zerihun, Y. T., Fenton, J. D. (2007). A Boussinesq-type model for flow over trapezoidal profile weirs. *J. Hydraul. Res.*, 45(4), 519–528.

Zerihun, Y. T. (2017a). A numerical study of non-hydrostatic shallow flows in open channels. *Arch. Hydro-Eng. Environ. Mech.*, 64(1), 17–35.

Zerihun, Y. T. (2017b). A non-hydrostatic depth-averaged model for hydraulically steep free-surface flows. *Fluids*, 2(4), https://doi.org/10.3390/fluids2040049.

Zerihun, Y. T. (2020). Free flow and discharge characteristics of trapezoidal-shaped weirs. *Fluids*, 5(4), https://doi.org/10.3390/fluids5040238.

Zerihun, Y. T. (2021a). Non-hydrostatic transitional open-channel flows from a supercritical to a subcritical state. *Slovak J. Civ. Eng.*, 29(2), 39–48.

Zerihun, Y. T. (2021b). On the numerical modeling of non-hydrostatic flows with dual free surfaces. *Water Util. J.*, 29, 29–42.

Zigrang, D. J., Sylvester, N. D. (1982). Explicit approximations to the solution of Colebrook's friction factor equation. *AIChE J.*, 28(3), 514–515.